



# Synthesis and characterization of the first soluble nonracemic chiral main-chain perylene tetracarboxylic diimide polymers

Chenming Xue, Minzhi Chen, Shi Jin\*

Center of Engineered Polymeric Materials, Department of Chemistry, College of Staten Island and Graduate Center, The City University of New York, Staten Island, NY 10314, USA

## ARTICLE INFO

### Article history:

Received 12 August 2008

Received in revised form 8 September 2008

Accepted 13 September 2008

Available online 2 October 2008

### Keywords:

Chiral

$\pi$ -Stack

Perylene tetracarboxylic diimide

## ABSTRACT

The first two nonracemic chiral main-chain perylene tetracarboxylic diimide (PDI) polymers have been synthesized via acyclic diene metathesis polymerization. The use of optically pure L- $\alpha$  amino acids as the starting materials enables us to tune PDI  $\pi$ -stacking interaction in optically active polymers. The integration of  $\pi$ -stack tuning groups renders two main-chain PDI polymers soluble in chloroform. Spectroscopic evidences suggest that PDI  $\pi$ -stacks form in chloroform solutions of the two PDI polymers, even at very low concentration, probably via an intra-molecular folding process. Inside  $\pi$ -stacks, PDI units organize in a left-handed helical fashion. Flexible free-standing films can be cast from chloroform solution of one polymer.

© 2008 Elsevier Ltd. All rights reserved.

## 1. Introduction

Perylene tetracarboxylic diimides (PDIs) have been attracting considerable attention as lightfast colorants [1–3], highly efficient fluorophores [4–6], the best *n*-type organic semiconductors [7–9] and versatile building blocks in self-assembly [10–14]. From the application point of view, incorporation of PDIs into main chains of polymeric architectures will generate mechanical robust materials with the attractive functionalities. One potentially exciting application of such a material is to replace expensive and poor film-forming fullerene derivatives as the electron acceptor and electron transport material in plastic solar cells. This calls for well-defined solution-processable main-chain PDI polymers with extensive  $\pi$ -stacked organization.

Although a number of PDI main-chain polymers have been reported [15–27], most of them [15,17,19,20,26,28] are only soluble in special solvents such as concentrated sulfuric acid or *m*-cresol, mainly due to the strong PDI  $\pi$ -stacking interaction. As a matter of fact, even many low molecular weight PDI dyes including some with long *n*-alkyl chains have very low solubility in common organic solvents [29–31]. To obtain better processability, two general approaches have been developed to reduce PDI  $\pi$ -stacking interaction and render low molecule weight PDIs readily soluble. The first approach involves the attachment of

solubilizing group to the carbocyclic scaffold (bay-area) [32–35]. Usually this modification leads to the distortion of the originally planar perylene ring so that the packing of PDI moieties becomes more difficult, which contributes to pronouncedly increased solubility. In the second approach the solubilizing groups are connected to the imide nitrogen atoms [4,6,36,37]. In this case, the planarity of the PDI core is retained. Among all solubilizing substituents, sterically demanding groups as 2,6-di-*tert*-butyl-phenyl [38] and long chain symmetrically secondary alkyl groups (swallow tails) [36] exhibited extraordinary ability to generate highly soluble PDI dyes, presumably because of the significantly reduced PDI  $\pi$ - $\pi$  interaction by a steric means. The first approach has been successfully implemented into the preparation of well soluble main-chain PDI polymers [16,18]. However, as far as charge transport is concerned, planarity of PDI rings is preferred for establishing PDI  $\pi$ -stacks as efficient charge transport pathways. Thus, functionalization at the imide nitrogen atoms is a preferred option. Along this line, highly flexible polyether [22,25] or highly branched hydrocarbon segments [27] have been incorporated into main-chain PDI polymers and oligomers affording soluble materials with planar PDI rings. Note that swallow tails have not been integrated to main-chain PDI polymers as solubilizing groups probably due to the difficulties in synthesis, although they have been extensively used in donor-acceptor dyads and triads [39–41], donor-bridge-acceptor molecules [42], fluorescent sensors and light switches [43–45], supramolecular assemblies [46,47], PDI multichromophores [48–50] and PDI side chain polymers [51–53]. Besides the

\* Corresponding author. Tel.: +1 718 982 3890; fax: +1 718 982 3910.  
E-mail address: [jin@mail.csi.cuny.edu](mailto:jin@mail.csi.cuny.edu) (S. Jin).

above-mentioned approaches initially developed for low molecular weight PDIs, copolymerization with other monomers has also been proven useful in giving soluble main-chain PDI polymers [17,20,21,23,24,26,28].

Recently we have found that the incorporation of a library of naturally-occurring  $\alpha$ -amino acids into PDIs offers an efficient way to tune  $\pi$ -stacking interaction between adjacent rigid units, mainly by steric effects [54,55]. This tunability is highly desired as it allows us to achieve a delicate balance between good solubility and the ability to form PDI  $\pi$ -stacks with extensive intermolecular  $\pi$  orbital overlap, which is crucial for various optoelectronic applications. When an optically pure  $\alpha$ -amino acid is used, nonracemic chiral PDI molecules result since the chirality centers do not participate in reactions. The configurational chirality may express as helical aggregates of PDI chromophores in a defined fashion, which could lead to increased charge carrier mobilities [9]. With the integration of the unique PDI  $\pi$ -stack tunability and the optical activity into polymers, we report the synthesis and characterization of the first solution-processable nonracemic chiral main-chain PDI polymers.

## 2. Experimental section

### 2.1. Instruments and characterization

All measurements were carried out at room temperature unless otherwise noted.  $^1\text{H}$  NMR and  $^{13}\text{C}$  NMR spectra were recorded on a Varian 300 MHz or 600 MHz NMR spectrometer with deuterated chloroform ( $\text{CDCl}_3$ ) as the solvent at 25 °C. For  $^1\text{H}$  NMR, the chemical shifts were reported using  $\text{CHCl}_3$  residue ( $\delta = 7.26$  ppm) in deuterated chloroform as the internal standard. For  $^{13}\text{C}$  NMR, the chemical shifts were reported using the  $\text{CDCl}_3$  signal ( $\delta = 77.16$  ppm) as the reference. Elemental analysis was carried out by Atlantic Microlab, Inc. Mass measurement was carried out by CUNY-Hunter MS center. The IR spectra were acquired on a Nicolet Magna 550 FTIR spectrometer at a resolution of  $2\text{ cm}^{-1}$ . UV–vis spectra were collected on a Varian UV–vis spectrometer at a resolution of 1 nm. Size exclusion chromatography analysis was carried out on an Alliance GPCV 2000 (Waters) instrument equipped with four Waters Styragel HR columns, i.e. HR-1, HR-3, HR-4, HR-5E. Measurements are relative to a calibration with polystyrene standards. HPLC grade THF was used as the eluent, at a flow rate of 1.0 mL/min at 30 °C. An UV–vis detector was used with the detection wavelength set to 527 nm. Circular dichroism spectra were obtained on the AVIV Circular Dichroism model 410 spectrometer at 25 °C with a bandwidth of 1 nm. The wavelength step was 1 nm and three scans were averaged for every spectrum. Electrochemistry measurements were performed with a three-electrode setup using a Princeton applied research M2273 potentiostat. Differential pulse voltammetry technique was employed. The pulse height and pulse width were 25 mV and 50 ms, respectively. The scan rate was 20 mV/s. A platinum wire and a silver wire electrode were employed as the counter electrode and the pseudo-reference electrode, respectively. The working electrode was a platinum disk with a diameter of 0.5 mm. Before each use, the working electrode was carefully polished using 0.3  $\mu\text{m}$  aluminum oxide polishing compound and cleaned in an ultrasonic bath with acetone. Argon was bubbled through the solutions to remove oxygen, and a slight argon overpressure was maintained during each measurement. The solvent was *o*-dichlorobenzene, and the supporting electrolyte was tetrabutylammonium tetrafluoroborate. The potential values were reported vs. the ferrocene/ferrocenium ( $\text{Fc}/\text{Fc}^+$ ) couple, as recommended by IUPAC [56].

### 2.2. Materials

All reagents and chemicals were purchased from Fisher scientific or VWR international and used as-received unless otherwise noted. Grubbs II catalyst was purchased from Sigma–Aldrich. 1, 2-Dichlorobenzene was distilled under a reduced pressure before use. Tetrabutylammonium tetrafluoroborate was dried overnight under vacuum at 80 °C.

### 2.3. Synthesis of *N,N'*-di((*S*)-1-carboxyethyl)-3,4:9,10-perylenetetracarboxyldiimide (PDI-L-Ala)

Into a 50 mL Schlenk flask were charged 1.87 g *L*-alanine (21 mmol), 3,4:9,10-perylenetetracarboxyldianhydride (PTCDA) 3.92 g (10 mmol), and imidazole (28 g). The mixture was purged with argon for 15 min before being heated at 120 °C until the reaction mixture was completely soluble in water. Subsequently, the reaction mixture was cooled to 90 °C. Deionized water was added under the protection of argon. The dark red solution was filtered to remove the trace amount of unreacted PTCDA. The solution was then acidified with 2 M HCl aqueous solution to a pH value of 3–4, the formed precipitate was collected by suction filtration and thoroughly washed with deionized water until the filtrate was neutral. The red solid was collected and dried at 75 °C in vacuum oven until constant weight. PDI-L-Ala 5.131 g (96%) was obtained as a dark red solid.

### 2.4. Synthesis of *N,N'*-di((*S*)-1-carboxyl-3-methylbutyl)-3,4:9,10-perylenetetracarboxyldiimide (PDI-L-Leu)

PDI-L-Leu was prepared using the same methodology as described for PDI-L-Ala, with *L*-leucine replacing *L*-alanine. PDI-L-Leu 6.00 g (97%) was obtained as a dark red solid.

### 2.5. Synthesis of *N,N'*-di((*S*)-2-(10-undecenoxy)-1-methyl-2-oxoethyl)-3,4:9,10-perylenetetracarboxyldiimide (ML-Ala11)

Into a  $\text{N}_2$ -purged 20 mL vial were charged 1 mmol PDI-L-Ala (MW: 534), 152 mg (1.1 mmol)  $\text{K}_2\text{CO}_3$  and 5.8 g DMF solution containing 580 mg (2.2 mmol) 18-crown-6. The mixture was stirred for 30 min at room temperature, forming a deep purple solution. A total of 583 mg (2.5 mmol) 11-bromo-1-undecene was then added to the solution. The reaction mixture was stirred in dark at room temperature under an Argon atmosphere for 24 h before being poured into 40 mL methanol. The orange crystalline precipitate was collected by centrifugation and dried at room temperature in a vacuum oven for 12 h. The crude product is purified by column chromatography on silica gel using 20/1 (v/v) chloroform/acetone as the eluent. Yield 0.760 g (90.6%) ML-Ala11 as a dark red solid.  $^1\text{H}$  NMR ( $\text{CDCl}_3$ , 300 MHz):  $\delta$  (ppm) = 8.60 (d,  $J = 8.01$  Hz, 4H, Ar), 8.45 (d,  $J = 8.1$  Hz, 4H, Ar), 5.67–5.82 (m, 2H,  $\text{NCH}(\text{COO})\text{CH}_3$  and  $\text{CH}=\text{CH}_2$ ), 4.87–4.97 (m, 4H,  $\text{CH}=\text{CH}_2$ ), 4.2 (m, 4H,  $(\text{COO})\text{CH}_2$ ), 1.91–1.98 (m, 4H,  $\text{CH}_2\text{CH}=\text{CH}_2$ ), 1.76 (d,  $J = 7.03$  Hz, 6H,  $\text{NCH}(\text{COO})\text{CH}_3$ ), 1.53–1.67 (m, 4H,  $(\text{COO})\text{CH}_2\text{CH}_2$ ), 1.16–1.3 (m, 24H,  $(\text{COO})\text{CH}_2\text{CH}_2(\text{CH}_2)_6$ ).  $^{13}\text{C}$  NMR ( $\text{CDCl}_3$ , 75 MHz):  $\delta$  (ppm) = 170.82 (ester  $\text{C}=\text{O}$ ), 163.12 (imide  $\text{C}=\text{O}$ ), 139.67 ( $\text{H}_2\text{C}=\text{CH}-$ ), 135.13 (Ar), 132.16 (Ar), 129.90 (Ar), 126.81 (Ar), 123.65 (Ar), 114.70 ( $\text{H}_2\text{C}=\text{CH}-$ ), 66.24 ( $(\text{COO})\text{CH}_2$ ), 50.17 ( $\text{NCH}(\text{COO})\text{CH}_3$ ), 34.33 ( $\text{CH}_2\text{CH}=\text{CH}_2$ ), 30.00 ( $\text{CH}_2$ ), 29.87 ( $\text{CH}_2$ ), 29.70 ( $\text{CH}_2$ ), 29.65 ( $\text{CH}_2$ ), 29.40 ( $\text{CH}_2$ ), 29.02 ( $\text{CH}_2$ ), 26.45 ( $\text{CH}_2$ ), 15.34 ( $\text{NCH}(\text{COO})(\text{CH}_3)$ ). FT-IR: 3077 (vinyl CH), 2925 (antisymmetric  $\text{CH}_2$ ), 2854 (symmetric  $\text{CH}_2$ ), 1746 (ester  $\text{C}=\text{O}$ ), 1700 (symmetric imide  $\text{C}=\text{O}$  symmetric), 1663 (antisymmetric imide  $\text{C}=\text{O}$ ), 1594 (aromatic ring stretch). HRMS ( $\text{M} + \text{H}$ ) $^+$ : Calcd for  $\text{C}_{52}\text{H}_{59}\text{N}_2\text{O}_8$  839.42714; Found: 839.42667.

### 2.6. Synthesis of N,N'-di((S)-2-(10-undecenoxy)-1-(2-methylpropyl)-2-oxoethyl)-3,4:9,10-perylenetetracarboxyldiimide (ML-Leu11)

ML-Leu11 was prepared and purified using the same methodology as described for ML-Ala11, with PDI-Leu replacing PDI-Ala. Yield ML-Leu 0.838 g (90.8%) as a dark red solid.  $^1\text{H NMR}$  ( $\text{CDCl}_3$ , 600 MHz):  $\delta$  (ppm) = 8.70 (d,  $J = 8.04$  Hz, 4H, Ar), 8.63 (d,  $J = 8.1$  Hz, 4H, Ar), 5.81–5.78 (m, 2H,  $\text{NCH}(\text{COO})\text{CH}_2\text{CH}(\text{CH}_3)_2$ ), 5.76–5.69 (m, 2H,  $\text{CH}=\text{CH}_2$ ), 4.94–4.87 (m, 4H,  $\text{CH}=\text{CH}_2$ ), 4.22–4.08 (m, 4H,  $(\text{COO})\text{CH}_2$ ), 2.29–2.12 (m, 4H,  $\text{NCH}(\text{COO})\text{CH}_2\text{CH}(\text{CH}_3)_2$ ), 1.91–1.95 (m, 4H,  $\text{CH}_2\text{CH}=\text{CH}_2$ ), 1.64–1.57 (m, 6H,  $\text{NCH}(\text{CH}_2\text{CH}(\text{CH}_3)_2)(\text{COO})\text{CH}_2\text{CH}_2(\text{CH}_2)_7\text{CH}=\text{CH}_2$ ), 1.27–1.11 (m, 24H,  $(\text{CH}_2)_6\text{CH}_2\text{CH}=\text{CH}_2$ ), 1.038 and 0.952 (d, d,  $J = 6.6$  Hz, 12H,  $\text{NCH}(\text{COO})\text{CH}_2\text{CH}(\text{CH}_3)_2$ ).  $^{13}\text{C NMR}$  ( $\text{CDCl}_3$ , 75 MHz):  $\delta$  (ppm) = 170.88 (ester C=O), 163.68 (imide C=O), 139.66 ( $\text{H}_2\text{C}=\text{CH}-$ ), 135.40 (Ar), 132.46 (Ar), 130.16 (Ar), 127.12 (Ar), 123.81 (Ar), 123.66 (Ar), 114.64 ( $\text{H}_2\text{C}=\text{CH}-$ ), 66.18 ( $(\text{COO})\text{CH}_2\text{CH}_2$ ), 52.98 ( $\text{NCH}(\text{COO})\text{CH}_2\text{CH}(\text{CH}_3)_2$ ), 38.64 ( $\text{NCH}(\text{COO})\text{CH}_2\text{CH}(\text{CH}_3)_2$ ), 34.29 ( $\text{CH}_2\text{CH}=\text{CH}_2$ ), 29.98 ( $\text{CH}_2$ ), 29.85 ( $\text{CH}_2$ ), 29.67 ( $\text{CH}_2$ ), 29.65 ( $\text{CH}_2$ ), 29.40 ( $\text{CH}_2$ ), 28.98 ( $\text{CH}_2$ ), 26.44 ( $\text{CH}_2$ ), 26.05 and 23.70 ( $\text{NCH}(\text{COO})\text{CH}_2\text{CH}(\text{CH}_3)_2$ ), 22.70 ( $\text{NCH}(\text{COO})\text{CH}_2\text{CH}(\text{CH}_3)_2$ ). FT-IR: 3077 (vinyl CH), 2927 (antisymmetric  $\text{CH}_2$ ), 2855 (symmetric  $\text{CH}_2$ ), 1742 (ester C=O), 1702 (symmetric imide C=O symmetric), 1664 (antisymmetric imide C=O), 1594 (aromatic ring stretch). HRMS ( $\text{M} + \text{H}$ ) $^+$ : Calcd for  $\text{C}_{58}\text{H}_{71}\text{N}_2\text{O}_8$  923.52104; Found: 923.52281.

### 2.7. Synthesis of PL-Ala11

A total of 100 mg ML-Ala11 and 1 mg Grubbs II catalyst were added into a tube containing 2 mL distilled 1,2-dichlorobenzene. The mixture was stirred for 72 h at 60 °C and continuously purged by  $\text{N}_2$ . Chloroform 20 mL was then added to the reaction mixture. The solution and the solid residue were separated by centrifugation. The solid residue was extracted three times using 20 mL chloroform at 60 °C. The chloroform solutions were combined and the volume was reduced to 20 mL before 100 mL methanol was added to precipitate the product. The crude product PL-Ala11 was collected by centrifugation and dried in vacuum at 75 °C. Grubbs II catalyst was removed by adding 1 mL  $\text{CH}_2\text{Cl}_2$  solution containing 20 mg tris(hydroxymethyl)phosphine and 20 mg triethylamine into PL-Ala11 chloroform solution [57]. After stirring for 20 min, the solution was filtered through a short silica gel column. The solution volume was reduced to 20 mL by evaporation before 100 mL methanol was added. The precipitated polymer was collected and dried in vacuum oven at room temperature for 12 h for further characterization. Yield PL-Ala11 64 mg (66%) as a red solid.  $^1\text{H NMR}$  (all peaks are broad) ( $\text{CDCl}_3$ , 300 MHz):  $\delta$  (ppm) = 8.69–7.92 (8H, Ar), 5.76 (2H,  $\text{NCH}(\text{COO})\text{CH}_3$ ), 5.27 (2H,  $\text{CH}=\text{CH}$ ), 4.24 (4H,  $(\text{COO})\text{CH}_2$ ), 1.86–1.59 (14H,  $\text{NCH}(\text{COO})(\text{CH}_3)\text{CH}_2\text{CH}_2(\text{CH}_2)_6\text{CH}_2\text{CH}=\text{CH}_2$ ), 1.19 (24H,  $(\text{COO})\text{CH}_2\text{CH}_2(\text{CH}_2)_6$ ). FT-IR: 2926 (antisymmetric  $\text{CH}_2$ ), 2853 (symmetric  $\text{CH}_2$ ), 1745 (ester C=O), 1701 (symmetric imide C=O symmetric), 1663 (antisymmetric imide C=O), 1594 (aromatic ring stretch). Anal. Calcd for  $\text{C}_{50}\text{H}_{54}\text{N}_2\text{O}_8$ : C, 74.05; H, 6.71; N, 3.45; O, 15.78. Found: C, 73.30; H, 6.61; N, 3.46.

### 2.8. Synthesis of PL-Leu11

ML-Leu11 and 1 mg Grubbs II catalyst were added into a tube containing 2 mL distilled 1,2-dichlorobenzene. The mixture was stirred for 72 h at 60 °C and continuously purged by  $\text{N}_2$ . After cooling the reaction mixture to room temperature, 10 mL chloroform was added to reaction mixture giving a homogenous solution. The crude product was obtained by precipitating in excess methanol. The catalyst was removed by adding 1 mL  $\text{CH}_2\text{Cl}_2$  solution containing 20 mg tris(hydroxymethyl)phosphine and 20 mg

triethylamine into PL-Leu11 chloroform solution. After stirring for 20 min, the solution was filtered through a short silica gel column. The red solid product was recovered by precipitating in excess methanol. After drying in vacuum at room temperature for 12 h, 46 mg (47%) PL-Leu11 was obtained as a red solid.  $^1\text{H NMR}$  ( $\text{CDCl}_3$ , 300 MHz):  $\delta$  (ppm) = 8.47–8.27 (broad, 8H, Ar), 5.83–5.78 (2H,  $\text{NCH}(\text{COO})\text{CH}_2\text{CH}(\text{CH}_3)_2$ ), 5.26 (broad, 2H,  $\text{CH}=\text{CH}$ ), 4.22–4.20 (m, 4H,  $(\text{COO})\text{CH}_2$ ), 2.32–2.10 (m, 4H,  $\text{NCH}(\text{COO})\text{CH}_2\text{CH}(\text{CH}_3)_2$ ), 1.85 (broad, 4H,  $\text{CH}_2\text{CH}=\text{CH}_2$ ), 1.63 (broad, 6H,  $\text{NCH}(\text{COO})(\text{CH}_2\text{CH}(\text{CH}_3)_2)\text{CH}_2\text{CH}_2(\text{CH}_2)_7\text{CH}=\text{CH}_2$ ), 1.25–1.16 (broad, 24H,  $(\text{CH}_2)_6\text{CH}_2\text{CH}=\text{CH}_2$ ), 1.041 and 0.966 (d, d,  $J = 6.6$  Hz,  $J = 6.3$  Hz, 12H,  $\text{NCH}(\text{COO})\text{CH}_2\text{CH}(\text{CH}_3)_2$ ). FT-IR: 2927 (antisymmetric  $\text{CH}_2$ ), 2854 (symmetric  $\text{CH}_2$ ), 1745 (ester C=O), 1701 (symmetric imide C=O symmetric), 1663 (antisymmetric imide C=O), 1594 (aromatic ring stretch). Anal. Calcd for  $\text{C}_{56}\text{H}_{66}\text{N}_2\text{O}_8$ : C, 75.14; H, 7.43; N, 3.13; O, 14.30. Found: C, 74.30; H, 7.40; N, 3.07.

### 2.9. Fractionation of PL-Leu11

A total of 15 mL THF were added to a 3 mL  $\text{CHCl}_3$  solution containing 16 mg PL-Leu11. The precipitate (PL-Leu11A, the high molecular weight part) was collected by suction filtration. The pink-red solution was evaporated to dryness affording PL-Leu11B (the low molecular weight part). Both components were dried in vacuum at room temperature for 12 h. A total of 12 mg PL-Leu11A and 4 mg PL-Leu11B were obtained.

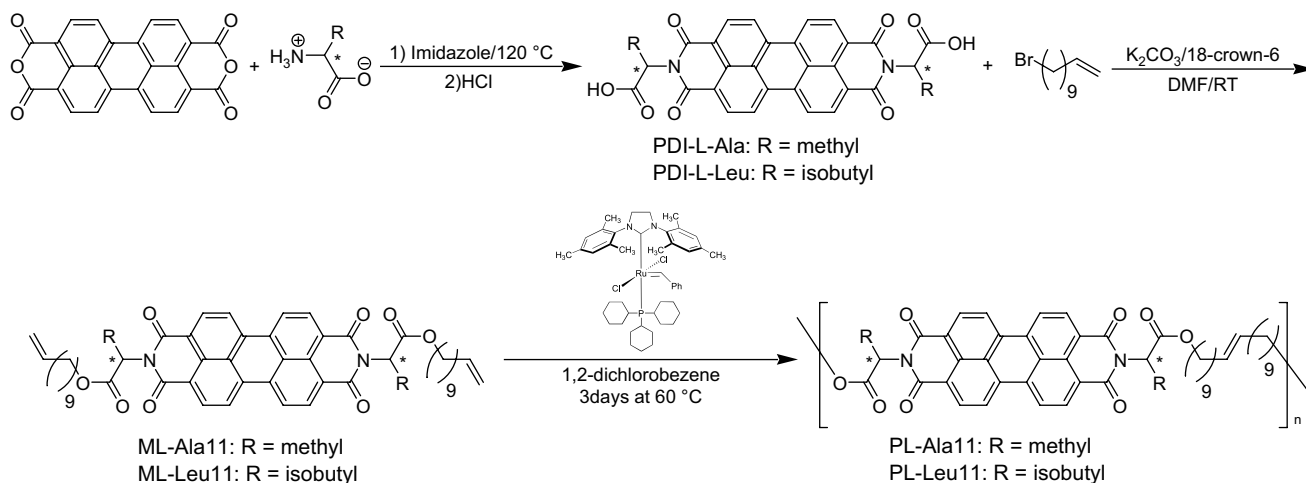
## 3. Results and discussion

PDI-L-Ala and PDI-L-Leu have been prepared in excellent yields by reacting perylene tetracarboxylic dianhydride with L-alanine and L-leucine in molten imidazole. The methyl group in PDI-L-Ala and the isobutyl group in PDI-L-Leu can be considered as the  $\pi$ -stack controlling groups that direct the formation of PDI  $\pi$  stacks by a steric means. Because isobutyl group is more sterically demanding than methyl group, it is expected that the formation of PDI  $\pi$ -stacks in PDI-L-Leu (and its derivatives) is more difficult than that in PDI-L-Ala, which should lead to higher solubility. To increase the processability, a long and flexible spacer is employed to connect the PDI units into semi-flexible main-chain polymers.

All labeled chirality centers are in S configuration.

Acyclic diene metathesis (ADMET) [58,59] was chosen to produce such semi-flexible polymers. ADMET has a few advantages over traditional polycondensation reactions. For instance, usually an ADMET reaction only involves one symmetrically substituted monomer equipped with two vinyl groups. Therefore, there is no need to take great care on stoichiometric balance as in an AA/BB polycondensation or carry out a multi-step synthesis to obtain the unsymmetrically substituted monomer as in an AB polycondensation. In addition, it is relatively easy to obtain clean final products since the ethylene gas is the only side product. In our case, one additional advantage of using ADMET is that the corresponding monomers, ML-Ala11 and ML-Leu11 exhibit high solubility in common organic solvents, which facilitates the preparation and purification of monomers, as well as the solution polymerization reactions. As shown in Scheme 1, the two monomers were synthesized in high yields from PDI-L-Ala and PDI-L-Leu, respectively.

Same as a conventional polycondensation reaction, an ADMET polymerization prefers high monomer concentration to minimize the formation of cyclic products, therefore, bulk polymerization is the top choice. However, because of the melting points of ML-Ala11 (186.5 °C) and ML-Leu11 (158.3 °C) are too high to support an efficient bulk ADMET reaction, solution polymerizations were performed. Since ADMET is an equilibrium process, removal of ethylene gas is needed to shift the equilibrium to the formation of



**Scheme 1.** ADMET synthesis of main-chain PDI polymers.

high molecular weight polymers. Usually this is achieved either by using a reduced pressure or purging the reactor with a nitrogen or argon flow. Here we chose to purge the reaction system with  $N_2$ . To prevent excessive loss of the solvent, 1,2-dichlorobenzene is chosen as the solvent because of its high boiling point ( $180\text{ }^\circ\text{C}$ ) and good ability to dissolve both monomers and the corresponding polymers. The polymerization reactions were catalyzed by Grubbs II catalyst with structure shown in Scheme 1.

ADMET of ML-Ala11 was first carried out. The original clear solution turned cloudy during the first day. This is probably due to the rapidly decreased solubility of the oligomers/cyclics of PL-Ala11 with the increased degree of polymerization. The reaction was stopped after three days.  $^1\text{H}$  NMR spectroscopy confirmed the quantitative conversion of the monomer to polymer and cyclic products. As shown in Fig. 1A, the vinyl group in the monomer displays its  $^1\text{H}$  resonance at about 5.7 (overlapped with  $H_1$ ) and about 4.9 ppm. After polymerization, the resonance peak at 4.9 ppm completely disappears and a new resonance peak appears at 5.3 ppm, indicating the formation of internal carbon–carbon double bonds. Completion of polymerization has also been verified by FT-IR as shown in Fig. 2A. The characteristic absorption bands of vinyl group of the monomer can be observed at  $3077$  and  $909\text{ cm}^{-1}$ . These bands disappeared after polymerization, signifying the complete conversion of the diene monomer.

ADMET of ML-Leu11 gave a viscous solution after 24 h and no precipitations were observed during the entire polymerization process, which implies that PL-Leu11 and corresponding macrocyclics are more soluble than PL-Ala11 in 1,2-dichlorobenzene, likely because the bulkier isobutyl group can better reduce PDI  $\pi$ -stacking interaction. The reaction was stopped after three days. The completion of reaction is also confirmed by  $^1\text{H}$  NMR and FT-IR in the same way as in the ADMET reaction of ML-Ala11, as shown in Figs. 1B and 2B.

PL-Ala11, is partially ( $\sim 85\%$ ) soluble in chloroform at about  $10^{-3}\text{ M}$  (in repeat units) concentration. The chloroform-soluble fraction is soluble partially in dichloromethane, THF, acetone, pyridine and ethyl acetate, producing a colored solution up to about  $10^{-5}\text{ M}$  concentrations. PL-Leu11 is completely soluble in chloroform at  $10^{-2}\text{ M}$  concentration. It also partially dissolves in dichloromethane, toluene, acetone at concentrations about  $10^{-5}\text{ M}$ . PL-Leu11's solubility in THF is very low, the concentration of the saturated solution at room temperature is about  $10^{-6}\text{ M}$ .

Molecular weights and their distribution of PL-Ala11 and PL-Leu11 were characterized by size exclusion chromatography (SEC). The extracted molecular weight data are given in Table 1. The

absorption coefficients of PL-Ala11 and PL-Leu11 at 527 nm are  $5.6 \times 10^4$  and  $6.5 \times 10^4\text{ L}/(\text{mol cm})$ , respectively. With such high extinction coefficients, we were able to record SEC traces with THF as eluent although both polymers exhibit low solubilities in this solvent. SEC curves of PL-Ala11 are presented in Fig. 3A. A series of

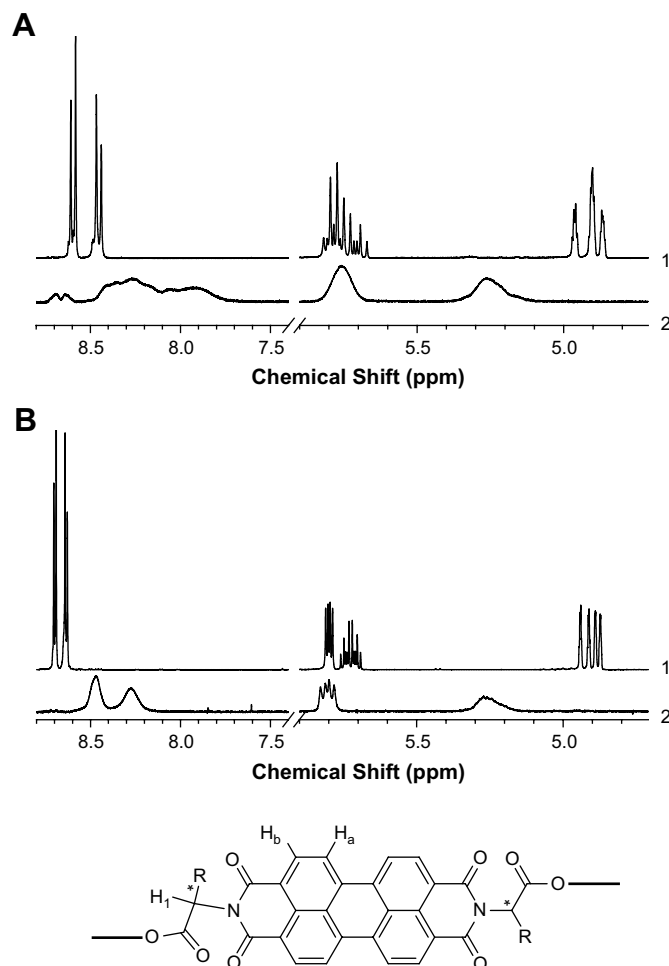


**Fig. 1.**  $^1\text{H}$  NMR spectra of ML-Ala11 (A1) and PL-Ala11 (A2); ML-Leu11 (B1) and PL-Leu11 (B2).



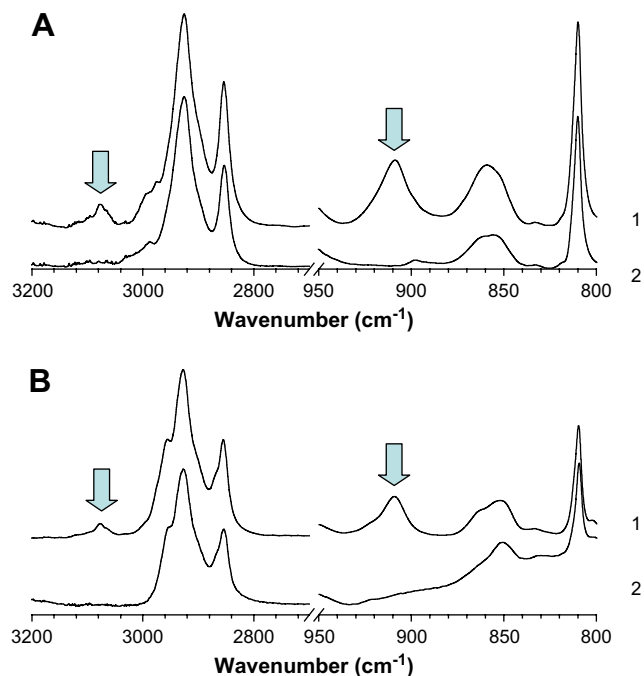


Fig. 2. FT-IR spectra of ML-Ala11 (A1) and PL-Ala11 (A2); ML-Leu11 (B1) and PL-Leu11 (B2). Absorption bands of vinyl groups were labeled with arrows.

Table 1  
Molecular weights and polydispersity of PDI polymers

Polymer	$M_n$ (g/mol)	$M_w$ (g/mol)	PDI
PL-Ala11	916	1470	1.60
PL-Leu11	810	1930	2.38
PL-Leu11A	3250	6920	2.13

sharp peaks with low molecular weights strongly suggest that PL-Ala11 is mainly a mixture of oligomers. Since no vinyl groups were observed in  $^1\text{H}$  NMR, these oligomers should possess a cyclic structure.

For PL-Leu11, as revealed by the SEC trace of the THF soluble part shown in Fig. 3B, also consists of mostly oligomers. However, because only a small part ( $\sim 25\%$ ) of PL-Leu11 is soluble in THF, the THF soluble part only represents the low molecular weight end of the material. To better understand the overall molecular weight distribution, a fractionation experiment was carried out by adding THF into concentrated PL-Leu11 chloroform solution. Although the precipitated fraction (PL-Leu11A) is essentially insoluble in THF, its saturated THF solution was able to give the SEC trace illustrated in Fig. 3C, thanks to PL-Leu11's high extinction coefficient at 527 nm. The number-average and weight-average molecular weights are 3300 and 6900 g/mol, respectively. It is reasonable to assume that THF is only able to dissolve the low molecular weight end of PL-Leu11A, thus the THF insoluble part must possess even higher molecular weight. Because the molecular weight measurements were relative to a calibration with polystyrene standards, the molecular weights of PDI polymers could be notably underestimated. This is due to the formation of PDI  $\pi$ -stacks in solution (see below), which reduces the hydrodynamic volume of a polymer chain. A reduced hydrodynamic volume corresponds to a decreased SEC molecular weight. The true high molecular weight nature of PL-Leu11 is firmly backed by the film-casting experiments. Flexible and free-standing films of PL-Leu11 can be drop-cast from its chloroform solution. One of such free-standing drop-cast films is shown in Fig. 4. They can be bent or folded without breaking, signifying the high molecular weight nature of PL-Leu11. In

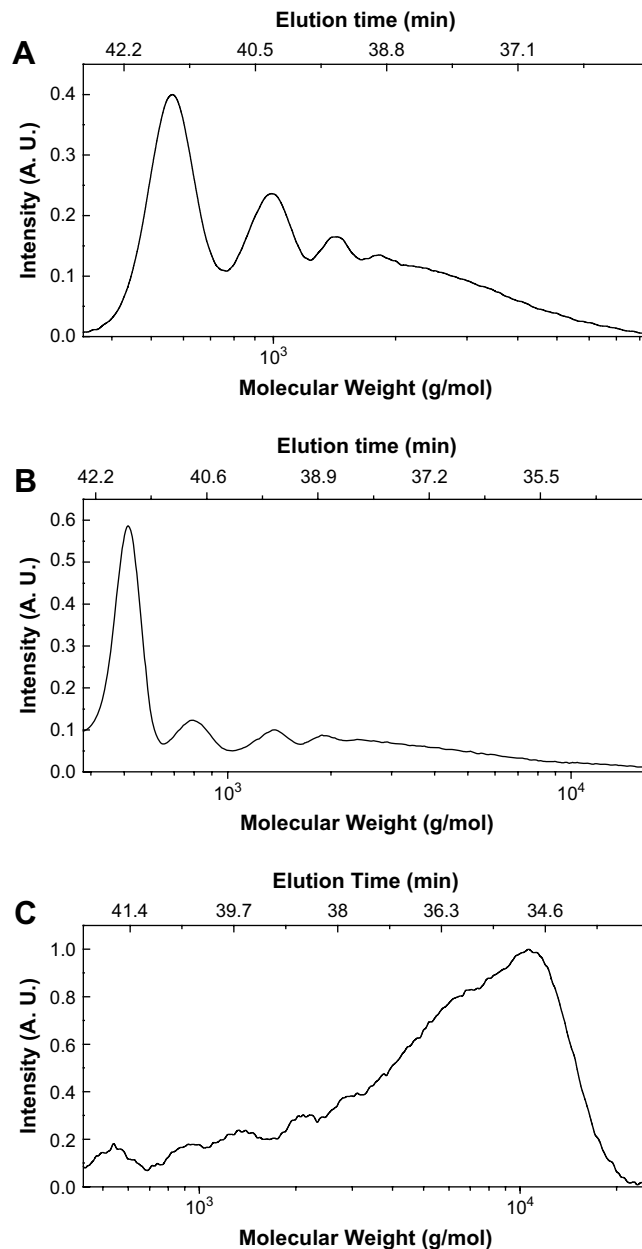


Fig. 3. SEC curves of PL-Ala11 (A), PL-Leu11 (B) and PL-Leu11A (C).

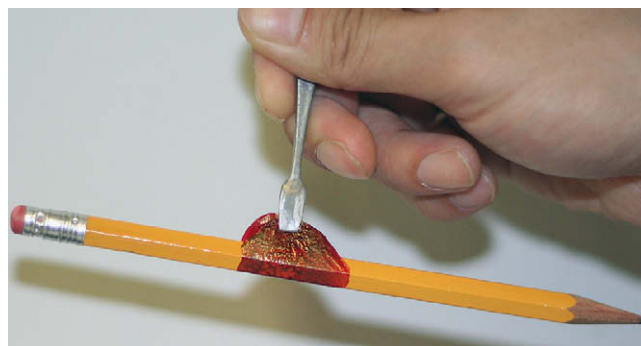


Fig. 4. The photograph of a PL-Leu11 film cast from chloroform solution. The film was used to wrap around a pencil and hang it in air.

contrast, the same procedure on PL-Ala11 produced a very brittle film that could not be lifted from the substrate, due to the substantially lower molecular weight.

Aggregation behavior of PL-Ala11, PL-Leu11 and their corresponding monomers were investigated by UV–visible (UV–vis) and circular dichroism (CD) spectroscopy. Aggregation of a PDI derivative in solution is strongly dependent upon the solvent–solute interaction. When the side chains are well solvated by the solvent, PDI  $\pi$ -stacking interaction becomes the major driving force of aggregation, resulting in the formation of PDI  $\pi$ -stacks. Due to the intermolecular  $\pi$ -orbital overlap in  $\pi$ -stacks, the electronic spectrum of stacked PDI units is different from that of unassociated chromophores [9,60–62]. UV–vis spectra of two monomers are shown in Fig. 5. The spectra of two monomers are essentially identical. The spectra feature a series of absorption peaks at 527, 490 and 458 nm. They can be attributed to the vibrational progression of the  $S_0 \rightarrow S_1$  electronic transition of the PDI monomers [61]. The absorption maximum at 527 nm originates from the transition from the zero vibrational level of the  $S_0$  state to the zero vibrational level of the  $S_1$  state ( $0 \rightarrow 0$ ). The peaks at 490 and 458 nm are due to the transition from the zero vibrational level of the  $S_0$  state to the first and second vibrational excited levels of the  $S_1$  state, respectively. They can be marked as  $0 \rightarrow 1$  (490 nm) and  $0 \rightarrow 2$  (458 nm). As reported earlier [25,61], the intensity ratio A527/A490 decreases upon the formation of  $\pi$ -stacks. For both monomers, A527/A490 = 1.68 at  $10^{-6}$  M concentration and this ratio changes very little when the concentration increases from 5.9  $\mu$ M to 9.6 mM. This implies that over such a broad concentration range, PDI molecules are essentially all in the monomeric state [25,61]. In contrast, A527/A490 changes appreciably when the concentration of bis-*N,N*-(2-(2-(2-(2-hydroxyethoxy)ethoxy)ethoxy)ethyl) perylene tetracarboxylic diimide chloroform solution changes from 0.48 to 7.7 mM [61]. This can be attributed to the existence of the  $\pi$ -stack tuning group in ML-Ala11 (methyl) and ML-Leu11 (isobutyl), thus it is more difficult for ML-Ala11 and ML-Leu11 to assemble into PDI  $\pi$ -stacks owing to greater steric hindrance toward the

formation of PDI  $\pi$ -stacks. Contrarily, the *N*-substituents in bis-*N,N*-(2-(2-(2-(2-hydroxyethoxy)ethoxy)ethoxy)ethyl) perylene tetracarboxylic diimide are much less sterically demanding.

The UV–vis spectrum of PL-Leu11 is illustrated in Fig. 5B. Similar to that of monomers, the spectrum changes little when the concentration increases from 5.9  $\mu$ M to 8.9 mM. However, the spectrum of the PL-Leu11 is considerably broader than that of ML-Leu11. In addition, A527/A490 for PL-Leu11 is about 1.46, which is clearly lower than 1.68 found for its monomer. Both the spectrum broadening and decreased A527/A490 value [25,61] suggest the existence of PDI  $\pi$ -stacks in PL-Leu11 solution, even at a concentration as low as 5.9  $\mu$ M. The organization of chromophore units in a PDI polymer is more complicated than monomeric PDIs. For a monomeric PDI, when concentration is the only variable, there is always a concentration below which the entropy contribution dominates and essentially all PDI molecules are in the unassociated state. However, for a polymer, even at an extremely low concentration, PDI  $\pi$ -stacks still can form via a folding process because a PDI chromophore has an appreciable probability to meet another PDI unit in the same polymer chain due to the chemical connectivity [25,62]. With the increasing concentration, folded PDI polymer chains could further self-assemble into larger aggregates. At  $\mu$ M concentration in chloroform, every PDI polymer chain can be considered to be well separated from each other, thus intramolecular  $\pi$ -stack formation or folding is the major form of aggregation. Although larger aggregates could form because of self-assembly of folded polymer chains, this was not observed for PL-Leu11 at concentrations up to 8.9 mM as evidenced by little change in UV–vis spectrum. The spectroscopic behavior of PL-Ala11 solution is essentially the same as that of PL-Leu11. The UV–vis spectrum shown in Fig. 5A suggests that PL-Ala11 chains also fold into PDI  $\pi$ -stacks in chloroform solution.

The formation of  $\pi$ -stacks in polymer solutions is also confirmed by solution  $^1\text{H}$  NMR experiments. The chemical shifts of  $H_a$  and  $H_b$  (Fig. 1) can be used to monitor  $\pi$ -stack formation of PDIs. Upon  $\pi$ -stack formation, both  $\delta_a$  and  $\delta_b$  decrease, accompanied by an increase of  $\delta_b - \delta_a$  [25,61,62]. For ML-Ala11, the perylene aromatic protons can be found as two doublets at  $\delta_a = 8.45$  and  $\delta_b = 8.6$ . At the same time, the corresponding protons appear at 7.92 and 8.26 ppm as two very broad peaks in PL-Ala11. The significantly decreased chemical shift values and the increased  $\delta_b - \delta_a$ , from 0.15 ppm in the monomer to 0.34 ppm in the polymer, strongly support the existence of PDI  $\pi$ -stacks in the polymer solution. In the aromatic region, there are two additional relative sharp, weak peaks at 8.64 and 8.69 ppm. They may be attributed to the perylene aromatic protons from the monocyclic PDI as a result of unimolecular ring-closing metathesis of the ML-Ala11. Similar behaviors were observed in  $^1\text{H}$  NMR spectra of ML-Leu11 and PL-Leu11. The perylene aromatic protons were observed at 8.63 and 8.7 ppm for ML-Leu11, while the corresponding protons appeared at 8.27 and 8.47 ppm as two broad peaks for PL-Leu11. However, the fact that no perylene proton peaks other than the two broad ones appeared in  $^1\text{H}$  NMR of PL-Leu11 implies that hardly any monocyclic PDI formed during polymerization.

When organizing into  $\pi$ -stacks, a PDI unit will either slip and/or rotate with respect to the adjacent PDI to minimize the energy [37,63,64]. If a rotation occurs, both left and right-handed rotations are possible. Nonchiral molecules must take the two rotation directions at the equal probability. Consequently, either no helical organization will be developed or right-handed and left-handed helices will form at the exactly same population. Contrarily, nonracemic chiral PDIs may favor a particular rotation direction over the other, leading to helically arranged chromophores with a well-defined handedness. ML-Ala11, ML-Leu11, PL-Ala11 and PL-Leu11 are nonracemic chiral materials because the optically pure amino acids were used as the starting

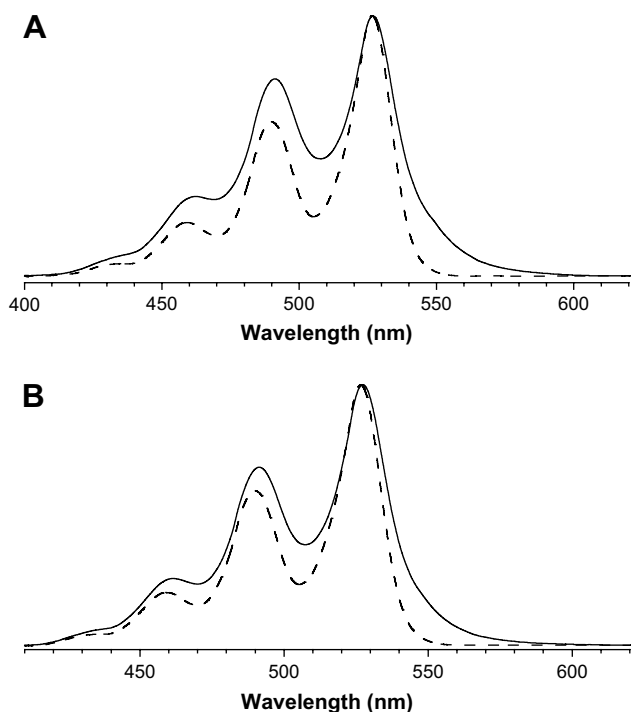


Fig. 5. UV–vis spectra of PL-Ala11 (solid) and ML-Ala11 (dash) (A); PL-Leu11 (solid) and ML-Leu11 (dash) (B). All solutions are at a concentration of 5.9  $\mu$ M in chloroform.

materials and the chirality centers are not involved in the reactions. As a result of the nonracemic chiral nature, a distinct helical arrangement of PDI units may exist in their  $\pi$ -stacks, which can be readily detected by CD spectroscopy. CD spectra of two polymers and their corresponding monomers are given in Fig. 6. No CD signals were observed for the monomers, whereas a pronounced CD signal was observed for both polymers with a positive maximum at 491 nm and a negative maximum at 548 nm. The bisignated CD signals are characteristic for helically stacked chromophores. The negative sign of the signal, which characterized by a positive to negative change with increasing wavelength, indicates the helical arrangement is left-handed [65].

Combining UV-vis,  $^1\text{H}$  NMR and CD results, a putative picture of aggregation behaviors of four PDIs in chloroform solution can be given. On one hand, the vast majority of monomer molecules exist in chloroform solution as the unassociated species, thus the configurational chirality does not express into a chiral arrangement of PDI molecules. On the other hand, PDI  $\pi$ -stacks form in polymers, even at a very low concentration, probably as the consequence of an intra-molecular folding process. Due to the nonracemic chiral nature of the polymers inherited from the L-form  $\alpha$  amino acids, the dye units favor the left-handed helical arrangement, which gave the negative bisignated CD signal. The schematic representation of such a helically folded polymer chain is depicted in Fig. 7.

Since PL-Leu11 can be fractionated, both fractions were subjected to UV and CD investigations to explore the molecular weight dependence of the aggregation behavior. The spectra were presented in Fig. 8. It appears that there are no significant differences between two fractions as far as the aggregation behavior is concerned. This suggests that PDI  $\pi$ -stacks formed as the consequence of the intra-molecular folding process are so disordered that a higher molecular weight does not make a noteworthy improvement in correlation of  $\pi$ -stacks. We speculate that

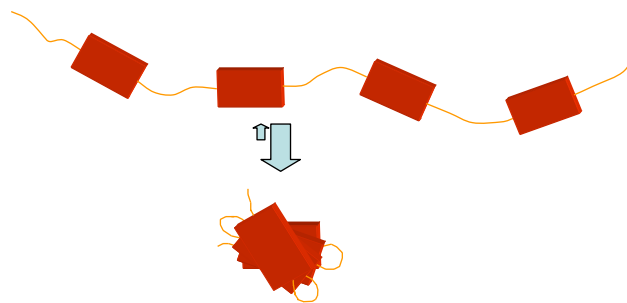


Fig. 7. The schematic representation of an extended polymer chain and its folded state.

the steric hindrance of the isobutyl group in PL-Leu11 is playing an important role here.

The ability of accepting electrons is among those important properties that make PDIs such useful materials. Electron-accepting ability of monomers and polymers was evaluated using differential pulsed voltammetry with  $\text{Fc}/\text{Fc}^+$  as the internal reference. As shown in Fig. 9, all PDIs undergo two reduction processes in a potential window between  $-0.9$  and  $-1.3$  V with the peak potential values given in Table 2. It is obvious that all four PDI derivatives exhibited the similar reduction potentials. This is because the imide nitrogen atoms are at the node of both highest occupied molecular orbital (HOMO) and lowest unoccupied molecular orbital (LUMO) wave functions of PDI, thus *N*-substitution has little effect on HOMO and LUMO levels. As a consequence, electrochemical property of PDIs is essentially independent on *N*-substitutions. The first reduction potential values ( $\sim -1.030$  V) of the two PDI polymers compare favorably with that of [6]-phenyl  $\text{C}_{61}$  butyric acid methyl ester (PCBM, a widely used electron acceptor in organic photovoltaics), which has a first reduction potential of  $-1.169$  V vs.  $\text{Fc}/\text{Fc}^+$  in 1,2-dichlorobenzene solution [66]. This suggests that these two PDI polymers possess similar electron-accepting power as PCBM. This fact, in addition to the

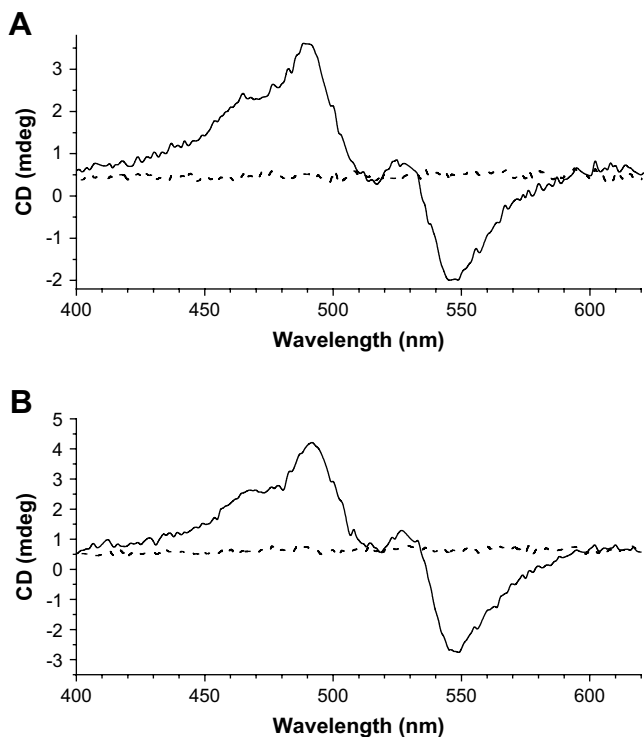


Fig. 6. CD spectra of PL-Ala11 (solid line) and ML-Ala11 (dash line) (A); PL-Leu11 (solid line) and ML-Leu11 (dash line) (B). All solutions are at a concentration of  $5.9 \mu\text{M}$  in chloroform.

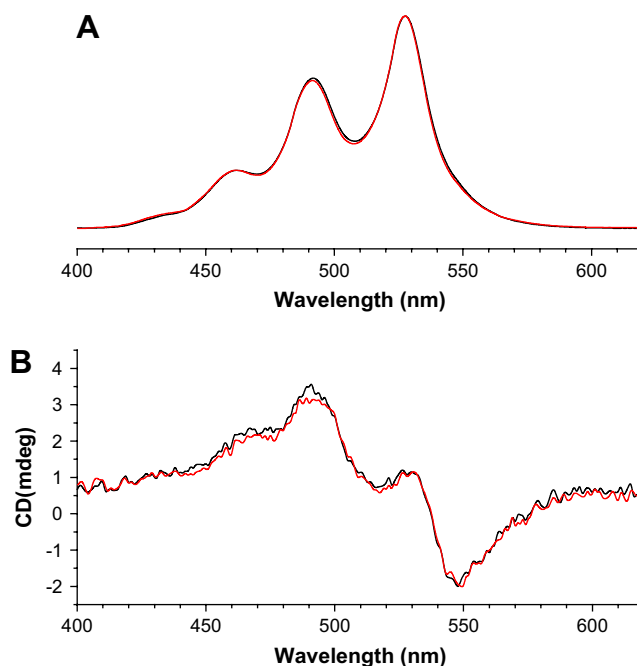


Fig. 8. UV (A) and CD (B) spectra of PL-Leu11A (black) and PL-Leu11B (red). All solutions are at a concentration of  $5.9 \mu\text{M}$  in chloroform. (For interpretation of the references to color in this figure legend, the reader is referred to the web version of this article.)

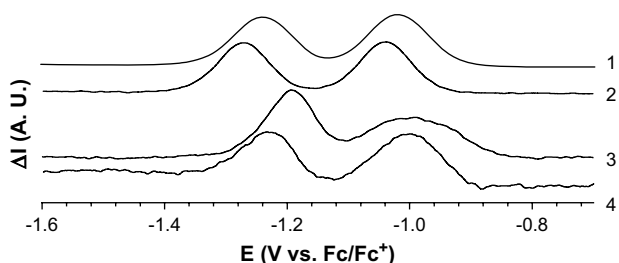


Fig. 9. Differential pulse voltammetry traces of ML-Ala11 (1); ML-Leu11 (2); PL-Ala11 (3) and PL-Leu11 (4).

Table 2

Reduction potentials of PDIs vs. Fc/Fc<sup>+</sup>

Compound	$E_1$ (V)	$E_2$ (V)
ML-Ala11	-1.020	-1.240
ML-Leu11	-1.038	-1.272
PL-Ala11	-1.000	-1.193
PL-Leu11	-1.004	-1.231

good film-forming ability of PL-Leu11, could make PL-Leu11 an attractive candidate as the electron acceptor in organic photovoltaic devices.

#### 4. Conclusions

The first two nonracemic chiral main-chain PDI polymers were synthesized via ADMET polymerization. They exhibited appreciable solubility in chloroform due to the existence of  $\pi$ -stack tuning groups. Intra-molecular PDI  $\pi$ -stack formation was observed in dilute polymer chloroform solutions. Inside  $\pi$ -stacks, PDI chromophores organize in a left-handed helical fashion. Free-standing and flexible films can be cast from PL-Leu11 chloroform solution. Good film-forming ability and strong electron affinity make PL-Leu11 a promising polymer for use in organic optoelectronic devices.

#### Acknowledgments

We thank Prof. Ralf M. Peetz and Dr. Narmandakh Mijid for SEC measurements. The authors also would like to thank Dr. Boris Arshava for assistance in CD measurements. This research was financially supported by the 3M Non-tenured Faculty grant and Petroleum Research Foundation. Partial support from PSC-CUNY Research Award Program is also gratefully acknowledged.

#### References

- Langhals H. *Heterocycles* 1995;40(1):477–500.
- Langhals H, Jona W, Einsiedl F, Wohnlich S. *Adv Mater* 1998;10(13):1022–4.
- Samudrala R, Zhang X, Wadkins RM, Mattern DL. *Bioorg Med Chem* 2007;15(1):186–93.
- Langhals H, Ismael R, Yuruk O. *Tetrahedron* 2000;56(30):5435–41.
- Langhals H, Karolin J, Johansson LB-A. *J Chem Soc Faraday Trans* 1998;94(19):2919–22.
- Rademacher A, Maerkele S, Langhals H. *Chem Ber* 1982;115(8):2927–34.
- Struijk CW, Sieval AB, Dakhorst JE, van Dijk M, Kimkes P, Koehorst RBM, et al. *J Am Chem Soc* 2000;122(45):11057–66.
- An ZS, Yu JS, Jones SC, Barlow S, Yoo S, Domercq B, et al. *Adv Mater* 2005;17(21):2580–3.
- Dehm V, Chen ZJ, Baumeister U, Prins P, Siebbeles LDA, Wurthner F. *Org Lett* 2007;9(6):1085–8.
- Wurthner F. *Chem Commun* 2004;(14):1564–79.
- Hoeben FJM, Jonkheijm P, Meijer EW, Schenning APH. *J Chem Rev* 2005;105(4):1491–546.
- Kelley RF, Shin WS, Rybtchinski B, Sinks LE, Wasielewski MR. *J Am Chem Soc* 2007;129(11):3173–81.
- Yagai S, Monma Y, Kawauchi N, Karatsu T, Kitamura A. *Org Lett* 2007;9(6):1137–40.
- Li X-Q, Stepanenko V, Chen Z, Prins P, Siebbeles LDA, Wuerthner F. *Chem Commun* 2006;(37):3871–3.
- Karayannidis G, Stamelos D, Bikiaris D. *Makromol Chem* 1993;194(10):2789–96.
- Dotcheva D, Klapper M, Müllen K. *Macromol Chem Phys* 1994;195(6):1905–11.
- Ghassemi H, Hay AS. *Macromolecules* 1994;27(15):4410–2.
- Quante H, Schlichting P, Rohr U, Geerts Y, Muellen K. *Macromol Chem Phys* 1996;197(12):4029–44.
- Icil H, Icli S. *J Polym Sci A Polym Chem* 1997;35(11):2137–42.
- Wang ZY, Qi Y, Gao JP, Sacripante GG, Sundararajan PR, Duff JD. *Macromolecules* 1998;31(7):2075–9.
- Mackinnon SM, Wang ZY. *J Polym Sci Polym Chem* 2000;38(19):3467–75.
- Neuteboom EE, Janssen RAJ, Meijer EW. *Synth Met* 2001;121(1–3):1283–4.
- Thelakkat M, Poesch P, Schmidt H-W. *Macromolecules* 2001;34(21):7441–7.
- Huang W, Yan D, Lu Q, Huang Y. *Eur Polym J* 2003;39(6):1099–104.
- Li ADQ, Wang W, Wang L-Q. *Chem Eur J* 2003;9(19):4594–601.
- Yao D, Sundararajan PR. *Eur Polym J* 2006;42(2):302–10.
- Yuney K, Icil H. *Eur Polym J* 2007;43(6):2308–20.
- Nielsen CB, Veldman D, Martin-Rapun R, Janssen RAJ. *Macromolecules* 2008;41(4):1094–103.
- Langhals H, Demmig S, Potrawa T. *J Prakt Chem* 1991;333(5):733–48.
- Sapagovas VJ, Gaidelis V, Kovalevskij V, Undzenas A. *Dyes Pigments* 2006;71(3):178–87.
- Balakrishnan K, Datar A, Naddo T, Huang J, Oitker R, Yen M, et al. *J Am Chem Soc* 2006;128(22):7390–8.
- Seybold G, Wagenblast G. *Dyes Pigments* 1989;11(4):303–17.
- Böhm A, Arms H, Henning G, Blaschka P. (BASF AG), Ger. Pat. Appl., DE 19,547,209 A1; 1997.
- Zhao Y, Wasielewski MR. *Tetrahedron Lett* 1999;40(39):7047–50.
- Lukas AS, Zhao Y, Miller SE, Wasielewski MR. *J Phys Chem B* 2002;106(6):1299–306.
- Demmig S, Langhals H. *Chem Ber* 1988;121(2):225–30.
- Wurthner F, Thalacker C, Diele S, Tschierske C. *Chem Eur J* 2001;7(10):2245–53.
- Lee SK, Zu Y, Herrmann A, Geerts Y, Muellen K, Bard AJ. *J Am Chem Soc* 1999;121(14):3513–20.
- Gomez R, Segura JL, Martin N. *Org Lett* 2005;7(4):717–20.
- Fukuzumi S, Ohkubo K, Ortiz J, Gutierrez AM, Fernandez-Lazaro F, Sastre-Santos A. *Chem Commun* 2005;(30):3814–6.
- Neuteboom EE, Meskers SCJ, Beckers EHA, Chopin S, Janssen RAJ. *J Phys Chem A* 2006;110(45):12363–71.
- Wescott LD, Mattern DL. *J Org Chem* 2003;68(26):10058–66.
- Mohr GJ, Spichiger UE, Jona W, Langhals H. *Anal Chem* 2000;72(5):1084–7.
- Zang L, Liu R, Holman MW, Nguyen KT, Adams DM. *J Am Chem Soc* 2002;124(36):10640–1.
- Fukaminato T, Irie M. *Adv Mater* 2006;18(24):3225–8.
- Neuteboom EE, Beckers EHA, Meskers SCJ, Meijer EW, Janssen RAJ. *Org Biomol Chem* 2003;1(1):198–203.
- Marcos Ramos A, Meskers SCJ, Beckers EHA, Prince RB, Brunsveld L, Janssen RAJ. *J Am Chem Soc* 2004;126(31):9630–44.
- Langhals H, Jona W. *Angew Chem Int Ed* 1998;37(7):952–5.
- Tauber MJ, Kelley RF, Giaimo JM, Rybtchinski B, Wasielewski MR. *J Am Chem Soc* 2006;128(6):1782–3.
- Holman MW, Liu R, Zang L, Yan P, DiBenedetto SA, Bowers RD, et al. *J Am Chem Soc* 2004;126(49):16126–33.
- Neuteboom EE, van Hal PA, Janssen RAJ. *Chem Eur J* 2004;10(16):3907–18.
- Lindner SM, Thelakkat M. *Macromolecules* 2004;37(24):8832–5.
- Hernando J, de Witte PAJ, van Dijk EMH, Korterk J, Nolte RJM, Rowan AE, et al. *Angew Chem Int Ed* 2004;43(31):4045–9.
- Xu YJ, Leng SW, Xue CM, Sun RK, Pan J, Ford J, et al. *Angew Chem Int Ed* 2007;46(21):3896–9.
- Sun RK, Xue CM, Owak M, Peetz RM, Jin S. *Tetrahedron Lett* 2007;48(38):6696–9.
- Gritzner G, Kuta J. *Pure Appl Chem* 1984;56(4):461–6.
- Maynard HD, Grubbs RH. *Tetrahedron Lett* 1999;40(22):4137–40.
- Wagener KB, Boncella JM, Nel JG. *Macromolecules* 1991;24(10):2649–57.
- Baughman TW, Wagener KB. *Metathesis polymerization*. *Adv Polym Sci* 2005;176:1–42.
- Ford WE. *J Photochem* 1987;37(1):189–204.
- Wang W, Han JJ, Wang LQ, Li LS, Shaw WJ, Li ADQ. *Nano Lett* 2003;3(4):455–8.
- Wang W, Li L-S, Helms G, Zhou H-H, Li ADQ. *J Am Chem Soc* 2003;125(5):1120–1.
- Klebe G, Graser F, Haedicke E, Berndt J. *Acta Crystallogr B* 1989;B45(1):69–77.
- Chen Z, Stepanenko V, Dehm V, Prins P, Siebbeles LA, Seibt J, et al. *Chem Eur J* 2007;13(2):436–49.
- Harada N, Nakanishi K. *Circular dichroism spectroscopy*. Oxford: Oxford University Press; 1983.
- Hummelen JC, Knight BW, LePeq F, Wudl F, Yao J, Wilkins CL. *J Org Chem* 1995;60(3):532–8.